Sustainable removal of chromium (III) from water using highly efficient magnetic biochar derived from Sawdust

American Journal of Chemistry
Vol. 11, No. 1, 1-12, 2026
e-ISSN:2616-5244

Ifeoma Juliet Opara[1]
Eno-Obong Sunday Nicholas[2]
Omale Agnes Umama[3]

(*Corresponding Author*)

[1,3]*Department of Chemistry, Faculty of Physical Sciences, Federal University Wukari, Taraba State, P.M.B.1020, Wukari, Nigeria.*
[1]*Email: j.opara@fuwukari.edu.ng*
[3]*Email: ifyuniquegreat@yahoo.com*
[2]*Department of Pure and Industrial Chemistry, Faculty of Physical Sciences, University of Nigeria, Nsukka, Nigeria.*
[2]*Email: eno-obong.nicholas.pg78610@unn.edu.ng*

ABSTRACT

In this study, magnetic biochars (MgSB450 and MgSB500) were applied for the adsorption of Cr^3 ions from aqueous solutions. FTIR analysis (PerkinElmer, USA) confirmed the presence of surface functional groups, including amine, hydroxyl (O-H), C=C, C-N, and C-H stretching of aliphatic groups. Adsorption experiments were conducted to evaluate the effects of contact time, pH, temperature, ionic strength, and initial metal ion concentration. Optimum adsorption was observed at pH 7, with removal efficiencies of 99.481 % and 99.404 % for MgSB450 and MgSB500, respectively. At an initial metal ion concentration of 80 mg/L, maximum adsorption of up to 99.98 % and 99.96 % for MgSB450 and MgSB500, respectively was obtained. It was noticed that as the temperature increases, the adsorption capacity decreases, and optimum adsorption (99.928 and 99.968 %) was observed at 30 °C for both MgSB450 and MgSB500. The results showed that as time increases, the removal efficiency of chromium ions increases for the first 30 min., and then gradually decrease with an increase in time for MgSB450. It reached a maximum adsorption of 99.848 %, while MgSB500 reached equilibrium at 50 mins., with an adsorption capacity of 98.208 %. From the results, it was observed that, the ionic strength increases, the adsorption capacity decreases, with maximum adsorption values of 95.772 % and 96.888 % for both adsorbents at a 0.4 % NaCl concentration. The sorption capacities of MgSB450 and MgSB500 were comparable, demonstrating strong potential for adsorbing chromium ions from aqueous solutions and their applicability in industrial wastewater treatment.

Keywords: *Adsorption, Chromium, Heavy metal, Magnetic biochar, FTIR, Removal efficiency.*

DOI: 10.55284/ajc.v11i1.1837
Citation | Opara, I. J., Nicholas, E.-O. S., & Umama, O. A. (2026). Sustainable removal of chromium (III) from water using highly efficient magnetic biochar derived from Sawdust. *American Journal of Chemistry, 11*(1), 1–12.

Funding: This study received no specific financial support.
Institutional Review Board Statement: Not applicable.
Transparency: The authors confirm that the manuscript is an honest, accurate, and transparent account of the study; that no vital features of the study have been omitted; and that any discrepancies from the study as planned have been explained. This study followed all ethical practices during writing.
Competing Interests: The authors declare that they have no competing interests.
Authors' Contributions: All authors contributed equally to the conception and design of the study. All authors have read and agreed to the published version of the manuscript.
History: Received: 25 December 2025/ Revised: 20 April 2026/ Accepted: 22 May 2026/ Published: 1 June 2026
Publisher: Online Science Publishing

Highlights of this paper

- Magnetic biochars (MgSB450 and MgSB500) were produced from waste biomass (Sawdust) for the adsorption of chromium ions.
- FTIR analysis (PerkinElmer, USA) confirmed the presence of surface functional groups, including amine, hydroxyl (O–H), C=C, C–N, and C–H stretching of aliphatic groups.
- The adsorption parameters, such as the effect of pH, contact time, temperature, ionic strength, and initial metal ion concentration for chromium ion adsorption, were determined, and the optimum removal efficiency of chromium up to 99.976% for MgSB450 and 99.908% for MgSB500 was obtained.

1. INTRODUCTION

The availability of safe and clean water is a fundamental requirement worldwide (Ruogu et al., 2025). One of the primary contributors to water pollution is the uncontrolled release of heavy metals from activities such as mining, battery manufacturing, and metal plating, as well as hazardous effluents containing organic matter and dyes from industries like textiles (Li et al., 2020; Ruogu et al., 2025; Zhao et al., 2025; Zhao et al., 2021). Heavy metals are naturally occurring elements in all ecosystems; nevertheless, excessive concentrations caused by human activity pose major environmental and health hazards (Wenzhe Gao et al., 2025; Ghodszad et al., 2021; Gong et al., 2024; Kayoumu et al., 2025; Kolton et al., 2011; Li et al., 2021; Liu et al., 2020; Xu et al., 2022). Heavy metals, even at minimal levels, are extremely harmful to aquatic ecosystems and humans due to their persistence, non-biodegradability, and tendency to bio-accumulate (Tianbao et al., 2025; Zahra et al., 2022). Rapid industrialization and urbanization have greatly increased heavy metal contamination due to the indiscriminate discharge of untreated industrial effluents (Eno-obong Nicholas et al., 2025; Khalil et al., 2012; Zhao et al., 2025). Mining, smelting, fossil fuel burning, waste incineration and industrial operations such as electroplating, metallurgy, and chemical manufacture are also major contributors (Feng et al., 2021; Kalsoom et al., 2024). Heavy metals such as Cr, Pb, Ni, Cd, As, Hg, and Cu disturb food systems and have been linked to neurological abnormalities, carcinogenic effects, and other chronic health concerns (Azadi & Raiesi, 2021; Fang et al., 2021; Weichun Gao et al., 2023; Hamid et al., 2020; Zhao et al., 2025).

Chromium is widely utilized in the leather tanning, electroplating, and dyeing sectors, and improper disposal causes significant environmental risks (Abbas et al., 2018; Naz et al., 2016; Zhang et al., 2015). It is mostly found as trivalent [Cr(III)] and hexavalent [Cr(VI)] species, both of which are highly soluble and bioavailable, with Cr(VI) being particularly hazardous and carcinogenic (Hamid et al., 2020; Qi et al., 2015; Zhang et al., 2015). As a result, removing chromium from wastewater has become a major environmental concern. Several treatment methods for heavy metal removal have been developed, including chemical precipitation, membrane processes, ion exchange, and electrochemical procedures (Zhang et al., 2019). Adsorption is particularly popular due to its operational simplicity, high efficiency, and cost-effectiveness. The objectives of this study were to evaluate the effects of contact time, temperature, ionic strength, initial metal ion concentration, and pH on the adsorption process using an adsorption experiment. Biochar made from biomass wastes like sawdust has recently acquired popularity as a low-cost and ecological adsorbent. Biochar can be chemically treated to improve surface functioning and metal binding capacity (Kaur et al., 2026; Ruogu et al., 2025). Magnetic biochar, in particular, generated by adding iron oxides during pyrolysis, has excellent adsorption capacity and is easier to recover after treatment, making it a potential material for removing chromium and other heavy metals from contaminated wastewater.

2. MATERIALS AND METHODS

2.1. Materials

Sample containers and apparatus used in this study were decontaminated with 10% HNO_3 solution, which was properly rinsed with distilled water many times immediately before usage, which was in line with the standard methods (Association of Official Analytical Chemists (AOAC), 1998). Reagents used in this research work were bought from commercial suppliers (Sigma Aldrich, USA) unless otherwise stated. Standard approved procedures were used to carry out the analyses to ensure the reliability and accuracy of the results according to the standard methods (Association of Official Analytical Chemists (AOAC), 1998).

2.2. Collection and Preparation of Biochar

Sawdust was collected from Wood Processing Sawmill Market in Wukari, Taraba State, Nigeria. The collected sample was washed, dried, pulverized, and later sieved using a mesh with a size of 2 mm to obtain a fine sawdust particle, which was then pyrolyzed at 450 °C and 500 °C to obtain biochar. The biochar obtained was designated with sample codes as SB450 and SB500, respectively as shown in Table 1.

2.3. Preparation and Modification of Magnetic Biochar

Magnetic biochar was produced following the method described by Liu et al., (2024). After modification, Sawdust was pyrolyzed at two different temperatures (450 °C and 500 °C) to produce biochar. The biochar produced was washed, ground, and sieved. To modify the biochar, a solution was prepared by mixing 10 g of biochar, 1.05 g of $FeSO_4.7H_2O$ and 1.05 g of $FeCl_3 \cdot 6H_2O$ into 50 ml of distilled water. In addition, 1.5M NaOH was mixed in 50 ml of distilled water. The solutions were mixed and stirred for 30 min. After that, the solution was put on the heater at 80 °C and stirred with a magnetic stirrer for 2 h. Then, it was pyrolyzed in a muffle furnace at 400 °C for 1 h. Finally, the magnetic biochar produced was washed several times with distilled water and was designated as MgSB450 and MgSB500, respectively.

2.3.1. Sample Codes, Names and Sources of the Sample

Samples used in this study for analysis was Magnetic Sawdust biochar which were pyrolyzed at 450 °C and 500 °C, respectively and were given sample codes as MgSB450 and MgSB500 as shown in Table 1.

Table 1. Sample codes, names with its sources.

S/N	Sample Code	Names and Sources of the Sample
1.	SB450	Sawdust biochar pyrolyzed at 450 °C
2.	SB500	Sawdust biochar pyrolyzed at 500 °C
3.	MgSB450	Magnetic Sawdust biochar pyrolyzed at 450 °C
4.	MgSB500	Magnetic Sawdust biochar pyrolyzed at 500 °C

2.4. The Fourier Transform Infrared Analysis (FTIR) on the Adsorbent

The surface functional groups of the synthesized magnetic biochar were characterized using Fourier transform infrared (FTIR) spectroscopy (PerkinElmer, USA). Prior to analysis, the magnetic biochar samples were thoroughly blended with infrared-grade potassium bromide (KBr, Sigma-Aldrich), previously dried at 110 °C for 24 h, in a mass ratio of 1mg sample to 10 mg KBr. The mixture was finely ground in an agate mortar to achieve uniform dispersion and subsequently compressed into transparent pellets. The FTIR spectra of 64 scans were recorded in the wavenumber range 4000 - 450 cm^{-1} with 4 cm^{-1} resolution.

2.5. Determination of Different Experimental Parameters on Adsorption Capacity

2.5.1. Effects of the Contact Time on Sorption Capacity

Sorption kinetics was evaluated by monitoring changes in metal ion uptake as a function of initial concentration over varying contact times. A fixed mass of magnetic biochar (0.1g) was contacted with 50 mL of chromium (III) [Cr^{3+}] solution and agitated continuously in a mechanical shaker for contact times ranging from 10 to 60 min. At predetermined intervals, the suspensions were withdrawn and filtered, and the residual metal ion concentration in the filtrate was quantified using a Spectra 220 Atomic Absorption Spectroscopy (AAS) (Ademoroti, 1996). The extent of metal uptake was evaluated based on the remaining Cr^{3+} concentration in solution determined (Osemeahon et al., 2016).

2.5.2. Effect of pH

The sorption capacity of magnetic biochar was investigated at different pH values (2, 5, 7, 8, and 12). 0.1M hydrochloric acid and 0.1M Sodium hydroxide were used to adjust the pH of the solution as needed. The residual metal ion was measured determined (Chamarthy et al., 2016).

2.5.3. Effect of Temperature on Sorption Capacity

The effect of temperature on the sorption capacity of the magnetic biochar was investigated. A dried sample (0.1g) was shaken with 50 mL of the metal ion solution. The synthetic wastewater was filtered and analyzed for residual metal ion concentration. This process was repeated at different temperatures, 30, 40, 50, 60, and 70 °C.

2.5.4. Effect of Ionic Strength on Sorption Capacity

The effect of ionic strength on sorption capacity was investigated using sodium chloride (NaCl) solutions at concentrations ranging from 0.1 to 2.0% (w/w). The adsorbent (0.2 g) was added to 50 cm^3 of each NaCl solution, and after equilibration, the residual metal ion concentration was evaluated.

2.5.5. Effect of Initial Ion Concentration

The effect of initial metal ion concentration on sorption capacity was investigated at 30 °C. A fixed dose of magnetic biochar (0.1g) was equilibrated with 50 mL of synthetic wastewater containing varying metal ion concentrations (20-100 mg L^{-1}) under continuous shaking. After equilibrium was attained, the suspensions were filtered, and the residual metal ion concentrations were determined (Osemeahon et al., 2016).

3. RESULTS AND DISCUSSION

The results obtained in this study for the effect of pH on adsorption capacity, initial metal ion concentration, temperature, ionic strength on sorption of metal ions and contact time on sorption capacity are shown in Tables 2-6 and Figures 1-5 while those of FTIR spectra for MgSB450 and MgSB500 are shown in Figures 6 and 7.

Table 2. Effect of pH on adsorption capacity.

S/N	Samples	pH Values	Metal Residue (%)	Removal Efficiency (%)
1.	MgSB450	2	20.596	79.404
2.	MgSB450	5	1.072	98.928
3.	MgSB450	7	0.520	99.480
4.	MgSB450	8	9.260	90.740
5.	MgSB450	12	0.624	99.376
6.	MgSB500	2	14.532	85.468
7.	MgSB500	5	5.176	94.824
8.	MgSB500	7	0.096	99.404
9.	MgSB500	8	4.812	95.188
10.	MgSB500	12	0.776	99.224

Table 3. Effect of initial metal ion concentration.

S/N	Samples	Concentration (mg/L)	Metal Residue (%)	Removal Efficiency (%)
1.	MgSB450	20	0.428	99.540
2.	MgSB450	40	0.012	99.572
3.	MgSB450	60	0.460	99.6448
4.	MgSB450	80	0.356	99.988
5.	MgSB450	100	0.296	99.704
6.	MgSB500	20	0.636	99.364
7.	MgSB500	40	0.032	99.648
8.	MgSB500	60	0.306	99.692
9.	MgSB500	80	0.204	99.968
10.	MgSB500	100	0.352	99.790

Table 4. Effect of Temperature.

S/N	Samples	Temperature (°C)	Metal Residue (%)	Removal Efficiency (%)
1.	MgSB450	30	0.360	99.928
2.	MgSB450	40	0.108	99.892
3.	MgSB450	50	0.072	99.740
4.	MgSB450	60	0.260	99.640
5.	MgSB450	70	1.540	98.460
6.	MgSB500	30	0.368	99.968
7.	MgSB500	40	0.032	99.768
8.	MgSB500	50	0.260	99.740
9.	MgSB500	60	0.608	99.632
10.	MgSB500	70	0.232	99.392

Table 5. Effect of ionic strength on sorption of metal ions.

S/N	Samples	Concentration (%)	Metal Residue (%)	Removal Efficiency (%)
1.	MgSB450	0.4	0.228	99.772
2.	MgSB450	0.8	0.092	99.908
3.	MgSB450	1.2	0.024	99.976
4.	MgSB450	1.6	0.096	99.904
5.	MgSB450	2.0	0.140	99.860
6.	MgSB500	0.4	0.112	99.888
7.	MgSB500	0.8	0.068	99.932
8.	MgSB500	1.2	0.092	99.908
9.	MgSB500	1.6	0.152	99.848
10.	MgSB500	2.0	0.264	99.736

Table 6. Effect of contact time on sorption capacity.

S/N	Samples	Time (min)	Metal Residue (%)	Removal Efficiency (%)
1.	MgSB450	10	1.688	98.312
2.	MgSB450	20	1.436	98.564
3.	MgSB450	30	0.152	99.848
4.	MgSB450	40	0.444	99.556
5.	MgSB450	50	0.728	99.272
6.	MgSB500	60	2.540	97.460
7.	MgSB500	10	7.832	90.380
8.	MgSB500	20	9.620	92.168
9.	MgSB500	30	3.724	95.572
10.	MgSB500	40	4.028	95.972

3.1. Effect of pH on Adsorption Capacity

Table 2 and Figure 1 represents the pH effect on the adsorption of Cr^{3+}. The pH value had a significant effect on the adsorption of metal, as it influences the electrostatic binding of ions. In the present study, this pH effect was carried out over the pH values 2, 5, 7, 8, and 12 at an initial concentration (25mg/L) of chromium. The removal efficiency of metals was maximum at pH 7 for both MgSB450°C and MgSB500°C, respectively. The metal uptake was observed to be 79.40 %, 98.92 %, 99.48 %, 90.74 %, and 99.38 % for MgSB450 °C and 85.47 %, 94.82 %, 99.40%, 95.19 % and 99.22 % for MgSB500 °C. It increased up to 99.48 % for MgSB450 °C and 99.40 % for MgSB500 °C at pH 7. At pH 2 the removal efficiency of both MgSB450 °C and MgSB500 °C was slightly lower (79.40 % for MgSB450 °C, 85.47% for MgSB500 °C). This trend could be due to protonation of active sites at low pH, protons and metal ions compete for the adsorption sites, and tend to decrease the sorption capacity. Adsorption also depends on the solubility of the adsorbate. Sorption increases with decreasing solubility and in most cases decreases with increasing pH. Adsorption increased with increasing pH (Shraddha & Singh, 2017), further increase in pH resulted in low solubility of Chromium, which may precipitate and not get adsorbed on the adsorbent surface.

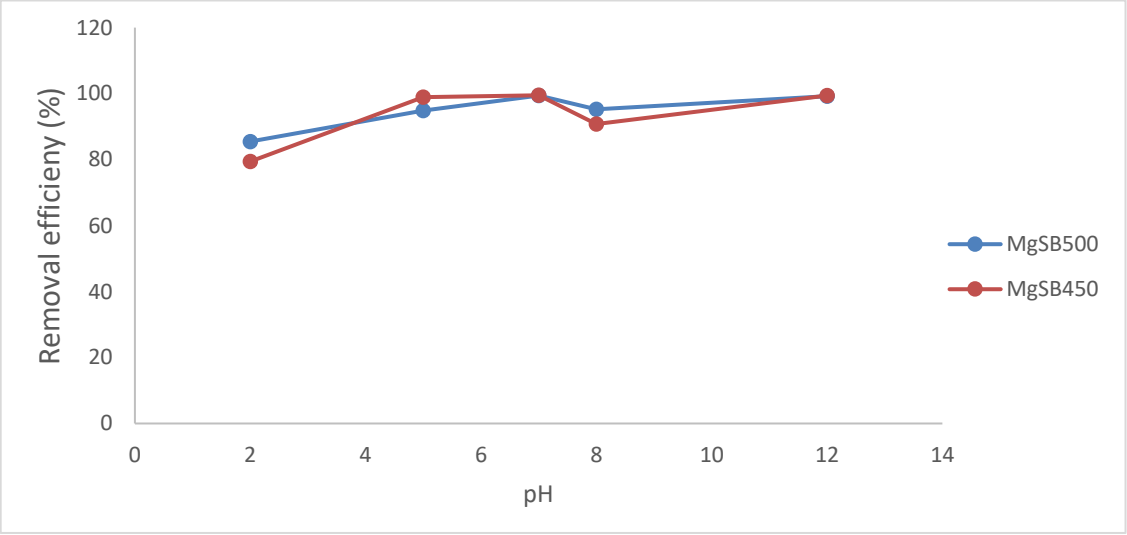

Figure 1. Effect of pH on adsorption of chromium ion.

3.2. Effect of Initial Metal Ion Concentration

As illustrated in Table 3 and Figure 2 above, the adsorption of Cr^{3+} ions was investigated over a range of initial concentrations (20-100 mg L^{-1}). The initial metal ion concentration serves as a key driving force for mass transfer between the aqueous phase and the adsorbent surface (Kailas & Wasewar, 2010). An increase in the initial

chromium concentration resulted in a corresponding rise in the amount of Cr^{3+} adsorbed, reflecting enhanced interaction between the metal ions and available surface sites. The adsorption rate and removal efficiency increased with concentration, reaching an optimum at 80 mg L^{-1} for both MgSB450 and MgSB500. This behaviour can be attributed to the higher availability of Cr^{3+}ions at the adsorbent interface. However, beyond this optimum concentration, a decline in removal efficiency was observed, likely due to saturation of active adsorption sites on the magnetic biochar surface.

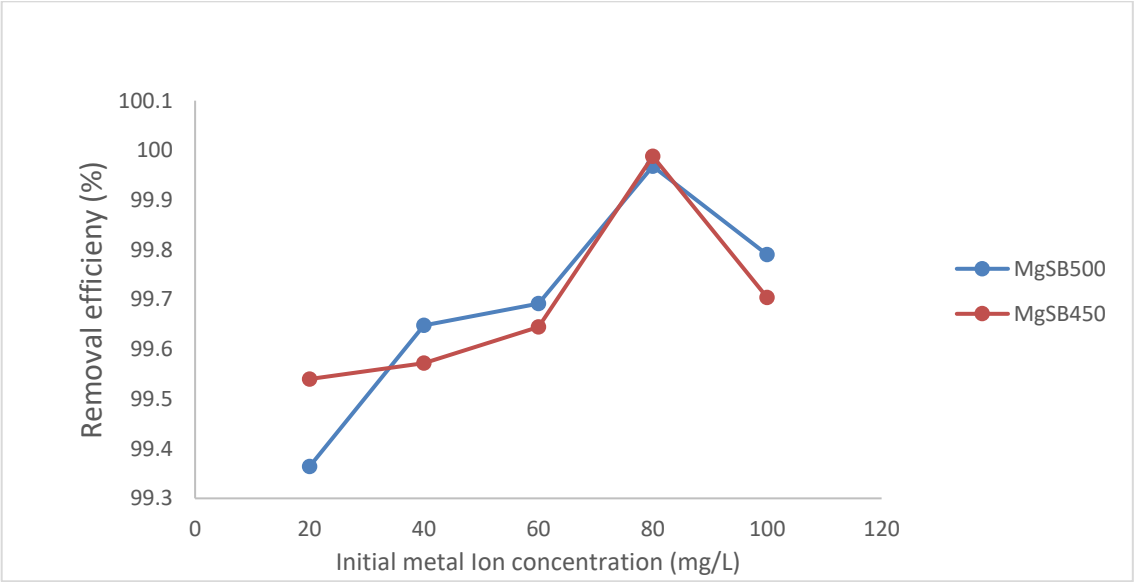

Figure 2. Effect of initial metal ion concentration on metal adsorption.

3.3. Effect of Temperature

Table 4 and Figure 3 above illustrate the effect of temperature on chromium ion removal. Adsorption experiments were conducted over a temperature range of 30-70 °C to evaluate the thermal influence on chromium uptake from aqueous solution. The results indicate that chromium removal efficiency decreased with increasing temperature, with maximum adsorption observed at 30 °C for both MgSB450 and MgSB500. The decline in removal efficiency at elevated temperatures may be attributed to structural changes in the adsorbent, such as reduced porosity and fewer available active sites, as well as enhanced desorption of chromium ions from the adsorbent surface at higher temperatures.

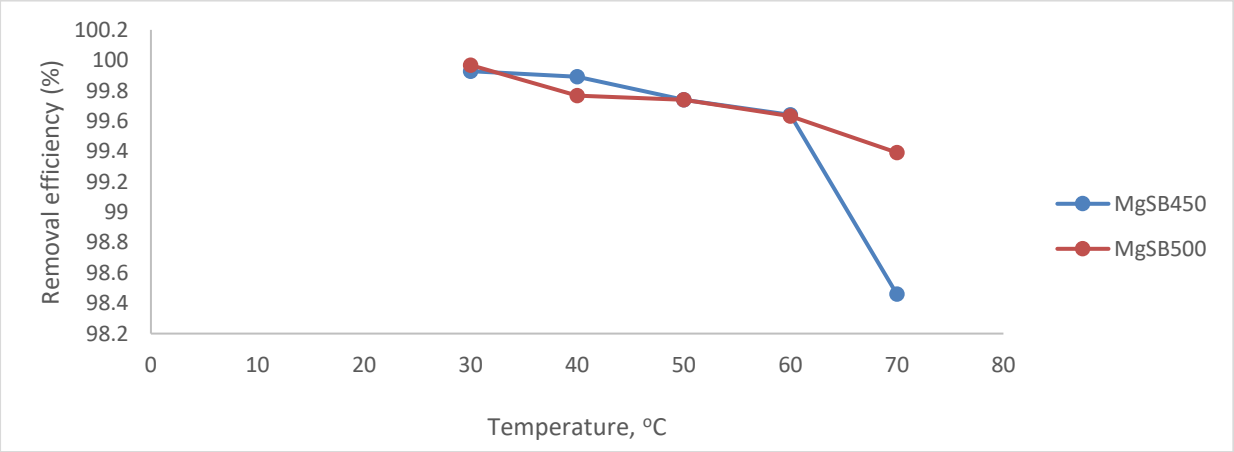

Figure 3. Effect of temperature (°C) on adsorption capacity.

3.4. Effect of Ionic Strength on Sorption of Metal Ions

Table 5 and Figure 4 above depict the effects of ionic strength on metal ion sorption. Dissolved salts are frequently found in natural waters and industrial effluents, and they might compete with target metal ions for accessible sorption sites on the adsorbent surface. Increased ionic strength lowers the activity of metal ions in solution by promoting non-ideal behaviour caused by increased electrostatic interactions and ion-pair formation. Because metal ion absorption is determined by its effective activity in solution, decreased activity leads to decreased adsorption onto the sorbent. As a result, as ionic strength increases, chromium ion sorption decreases due to increased competition between sodium and chromium ions for active binding sites on the adsorbent. The optimum adsorption capacity (95.772 % and 96.888 %) was observed at 0.4 % of NaCl for MgSB450 and MgSB500, respectively.

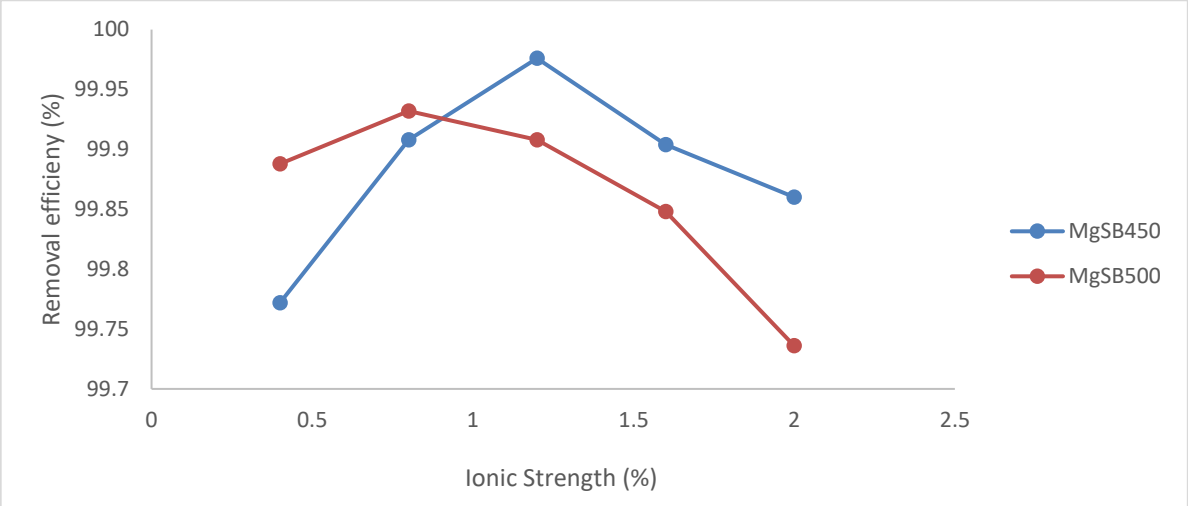

Figure 4. Effect of ionic strength on adsorption capacity.

3.5. Effect of Contact Time on Sorption Capacity

The results depicted in Table 6 and Figure 5 above indicate that Cr^{3+}adsorption onto the magnetic biochar was initially rapid, reaching equilibrium at 30 min for MgSB450 and 50 min for MgSB500. Metal uptake increased sharply during the early stages of contact, followed by a slower approach to equilibrium observed at 40 min and 60 min for MgSB450 and MgSB500, respectively. The rapid initial adsorption can be attributed to the diffusion of Cr^{3} ions onto the highly porous sorbent surfaces, where the abundant binding sites and large surface area facilitate efficient metal ion attachment. As the process progressed, the adsorption rate decreased, likely due to the progressive saturation of active sites on the adsorbent (Aishatu & Barminas, 2015). This behaviour reflects the typical sorption kinetics where initial uptake is dominated by surface interactions, while the later stages are controlled by the availability of residual binding sites.

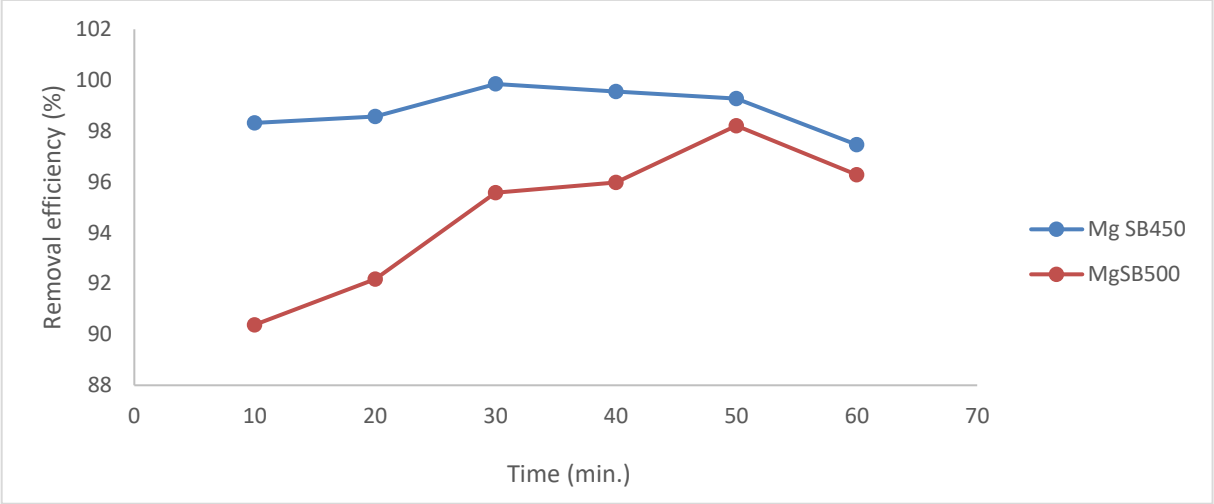

Figure 5. Effect of contact time on adsorption capacity.

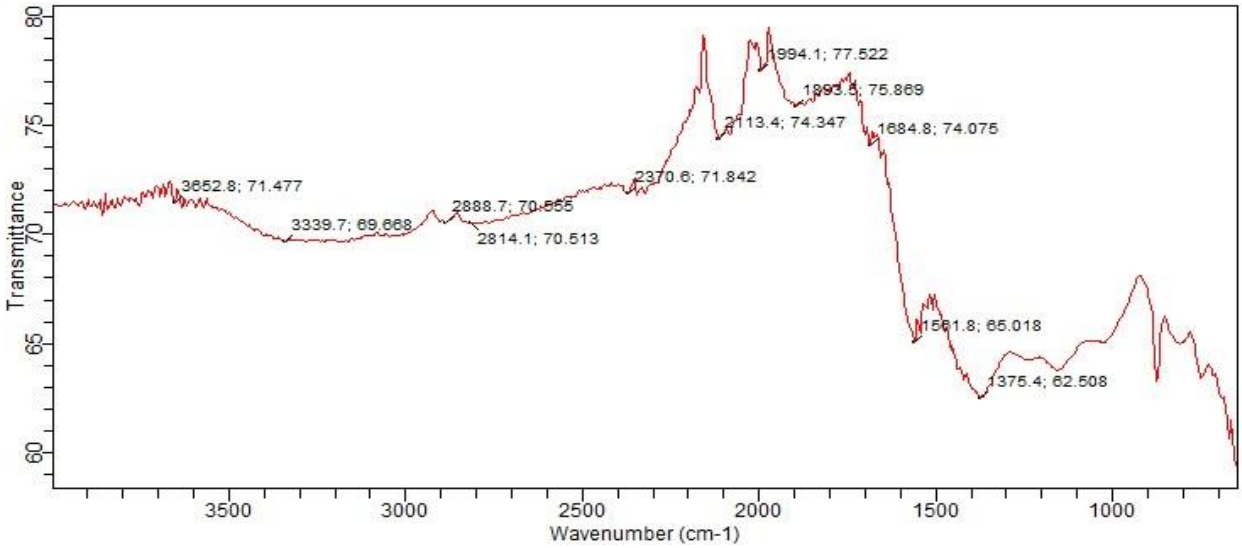

Figure 6. FTIR spectra for MgSB450.

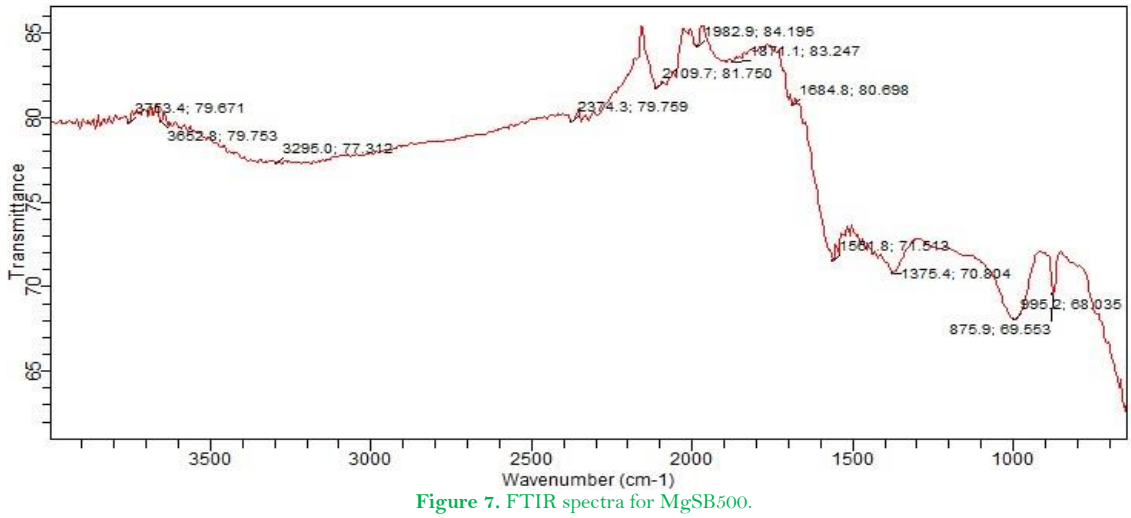

Figure 7. FTIR spectra for MgSB500.

3.6. Results of FTIR Spectra of MgSB450 and MgSB500

Figures 6 and 7 as shown above, present the FTIR spectra of MgSB450 and MgSB500, highlighting the functional groups on their surfaces. Peaks at 3652.8 cm^{-1} and 3763.4 cm^{-1} correspond to N–H stretching of amine

groups, while bands at 3339.7 cm^{-1} and 3295 cm^{-1} indicate O–H stretching of alcohol groups for MgSB450 and MgSB500, respectively. The C–H stretching of aliphatic groups is observed at 2814.1 cm^{-1} and 2374.3 cm^{-1}, and C=C stretching at 2113.4 cm^{-1} and 2109.7 cm^{-1} suggests the presence of alkenes. Peaks at 1561.8 cm^{-1} and 1581.8 cm^{-1} are attributed to C–N stretching of amide (II) groups, while the bands at 1375.4 cm^{-1} correspond to aromatic amines in both samples. The presence of these functional groups, particularly amine and hydroxyl groups, enhances the adsorption capacity of the magnetic biochar, as reflected in their high metal removal efficiency.

4. CONCLUSION

The synthesized magnetic biochar exhibited a highly porous structure and surface functional groups that promoted efficient metal-ion sorption. Adsorption experiments demonstrated excellent performance, with maximum removal efficiencies of 99.98 % and 99.96 % achieved at an initial Cr^{3+}concentration of 80 mg L^{-1} for MgSB450 and MgSB500, respectively. These results indicate that the prepared magnetic biochar is highly effective for chromium removal from aqueous solutions and holds significant potential for application in the treatment of industrial effluents.

REFERENCES

Abbas, Z., Ali, S., Rizwan, M., Zaheer, I. E., Malik, A., Riaz, M. A., Shalid, M. R., Rehman, M.Z., Al-Wabel, M. I. (2018). A critical review of mechanisms involved in the adsorption of organic and inorganic contaminants through biochar. Arabian Journal of Geosciences, *11*(16), 448. https://doi.org/10.1007/s12517-018-3790-1

Ademoroti, C. M. A. (1996). Environmental chemistry and toxicology. In (pp. 79-121). Ibadan: Fodulex Press Ltd.

Aishatu, H. S., & Barminas, J. T. (2015). Biosorption capacity of Lonchocarpus laxiflorus leaves biomass for adsorption of metal ions (Fe^{3+}, Pb^{2+}, Cr^{2+}, Cd^{2+}, and Ni^{2+}) from aqueous solution. International Journal of Scientific and Research Publications, *5*(1), 1–8.

Association of Official Analytical Chemists (AOAC). (1998). *Official method of analysis*. Washington, DC: Association of Official Analytical Chemists.

Azadi, N., & Raiesi, F. (2021). Biochar alleviates metal toxicity and improves microbial community functions in a soil co-contaminated with cadmium and lead. Biochar, *3*(4), 485-498. https://doi.org/10.1007/s42773-021-00123-0

Chamarthy, S., Seo, C. W., & Marshall, W. E. (2001). Adsorption of selected toxic metals by modified peanut shells. Journal of Chemical Technology & Biotechnology: International Research in Process, Environmental & Clean Technology, *76*(6), 593-597. https://doi.org/10.1002/jctb.418

Eno-obong S. Nicholas, Okudo, C. C., & Ukoha, P. O. (2025). Water quality index assessment of toxicity in direct and roofs runoff rainwater in industrial and remote areas of Eastern Nigeria. Scientific Reports, *15*(1), 36068. https://doi.org/10.1038/s41598-025-19983-8

Fang, D.D., Zhang, L.Z., & Wang, Q. (2021). Effects of superparamagnetic nanomaterials on soil microorganisms and enzymes in cadmium-contaminated paddy fields. Huan Jing ke Xue= Huanjing Kexue, *42*(3), 1523-1534.

Feng, H.L., Xu, C.S., He, H.H., Zeng, Q., Chen, N., Li, X.L., Ren, T.B., Ji, X.M., Liu, G.S. (2021). Effect of biochar on soil enzyme activity & the bacterial community and its mechanism. Huan Jing ke Xue= Huanjing Kexue, *42*(1), 422-432. https://doi.org/10.13227/j.hjkx.202005285.

Gao, W., He, W., Zhang, J., Chen, Y., Zhang, Z., Yang, Y., & He, Z. (2023). Effects of biochar-based materials on nickel adsorption and bioavailability in soil. Scientific Reports, *13*(1), 5880. https://doi.org/10.1038/s41598-023-32502-x

Gao, W., Li, Y., Luo, J., Wang, Y., Gao, W., Liu, X., & Li, T. (2025). Soil cadmium pollution decreases phosphorus-mineralizing microbial diversity and reduces phosphorus availability. Environmental Pollution, *371*, 125960. https://doi.org/10.1016/j.envpol.2025.125960

Ghodszad, L., Reyhanitabar, A., & Oustan, S. (2021). Biochar effects on phosphorus sorption-desorption kinetics in soils with dissimilar acidity. Arabian Journal of Geosciences, *14*(5), 366. https://doi.org/10.1007/s12517-021-06629-y

Gong, X., Xu, L., Langwig, M. V., Chen, Z., Huang, S., Zhao, D., Su, L., Zhang, Y., Francis, C.A., Li, J., & Baker, B. J. (2024). Globally distributed marine Gemmatimonadota have unique genomic potentials. Microbiome, *12*(1), 149. https://doi.org/10.1186/s40168-024-01871-4

Hamid, Y., Tang, L., Hussain, B., Usman, M., Lin, Q., Rashid, M. S., He, Z., Yang, X. (2020). Organic soil additives for the remediation of cadmium contaminated soils and their impact on the soil-plant system: A review. Science of the Total Environment, *707*, 136121. https://doi.org/10.1016/j.scitotenv.2019.136121

Kailas, L., & Wasewar. (2010). Adsorption of metals onto tea factory waste: A review. International Journal of Recent Research and Applied Studies, *3*(3), 303–322.

Kalsoom, Ali, A., Khan, S., Ali, N., & Khan, M. A. (2024). Enhanced ultrasonic adsorption of pesticides onto the optimized surface area of activated carbon and biochar: adsorption isotherm, kinetics, and thermodynamics. Biomass Conversion and Biorefinery, *14*(14), 15519-15534. https://doi.org/10.1007/s13399-023-04170-4

Kaur, K., Saleem, M., & Kaur, H. (2026). Biochar and biopolymer based nanomaterials for microplastic remediation: a sustainable approach for environment. Topics in Catalysis, *69*(4), 825-852. https://doi.org/10.1007/s11244-025-02185-x

Kayoumu, M., Wang, H., & Duan, G. (2025). Interactions between microbial extracellular polymeric substances and biochar, and their potential applications: A review. Biochar, *7*(1), 62. https://doi.org/10.1007/s42773-025-00452-4

Khalil Ahmad, K. A., Bhatti, I., Majid Muneer, M. M., Munawar Iqbal, M. I., & Zafar Iqbal, Z. I. (2012). Removal of heavy metals (Zn, Cr, Pb, Cd, Cu and Fe) in aqueous media by calcium carbonate as an adsorbent. International Journal of Chemical and Biochemical Sciences, *2*, 48–53.

Kolton, M., Meller Harel, Y., Pasternak, Z., Graber, E. R., Elad, Y., & Cytryn, E. (2011). Impact of biochar application to soil on the root-associated bacterial community structure of fully developed greenhouse pepper plants. Applied and Environmental Microbiology, *77*(14), 4924-4930.

Li, X., Lu, X., Nie, S., Liang, M., Yu, Z., Duan, B., . . . Si, C. (2020). Efficient catalytic production of biomass-derived levulinic acid over phosphotungstic acid in deep eutectic solvent. Industrial Crops and Products, *145*, 112154. https://doi.org/10.1016/j.indcrop.2020.112154

Li, Y., Yu, H., Liu, L., & Yu, H. (2021). Application of co-pyrolysis biochar for the adsorption and immobilization of heavy metals in contaminated environmental substrates. Journal of Hazardous Materials, *420*, 126655. https://doi.org/10.1016/j.jhazmat.2021.126655

Liu, B., Wu, Y., Xing, Z., Zhang, J., & Xue, Y. (2024). Optimization of magnetic biochar preparation process, based on methylene blue adsorption. Molecules, *29*(21), 5213. https://doi.org/10.3390/molecules29215213

Liu, G., Meng, J., Huang, Y., Dai, Z., Tang, C., & Xu, J. (2020). Effects of carbide slag, lodestone and biochar on the immobilization, plant uptake and translocation of As and Cd in a contaminated paddy soil. Environmental Pollution, *266*, 115194. https://doi.org/10.1016/j.envpol.2020.115194

Naz, A., Mishra, B. K., & Gupta, S. K. (2016). Human health risk assessment of chromium in drinking water: a case study of Sukinda chromite mine, Odisha, India. Exposure and Health, *8*(2), 253-264. https://doi.org/10.1007/s12403-016-0199-5

Osemeahon, S., Kolo, A., Opara, I., & Hamma, A. (2016). Bioremediation of wastewater with immobilized dargaza (Grewia mollis): effect of some physical properties. IOSR Journal of Applied Chemistry, *9*, 37-43.

Qi, Y., Jiang, M., Cui, Y.-L., Zhao, L., & Liu, S. (2015). Novel reduction of Cr (VI) from wastewater using a naturally derived microcapsule loaded with rutin–Cr (III) complex. Journal of Hazardous Materials, *285*, 336-345.

Ruogu, T., Qiu, S., Wu, C., & Tan, J. (2025). Biochar: From agricultural waste byproducts to novel adsorbents for ammonia and micro/nanoplastics (MNPs). Biochar, *7*(1), 122. https://doi.org/10.1007/s42773-025-00554-z

Shraddha, R. S., & Singh, A. (2017). Adsorption of heavy metals from waste waters using waste biomass. International Journal of Engineering Research & Technology, *6*(1), 423-428.

Tianbao, R., Feng, H., Wan Mahari, W. A., Yun, F., Li, M., Ma, N. L., Cai X., Liu, G., Liew, R. K., & Lam, S. S. (2025). Biochar and microbial synergy: Enhancing tobacco plant resistance and soil remediation under cadmium stress. Biochar, *7*(1), 119. https://doi.org/10.1007/s42773-025-00535-2

Xu, H., Wang, B., Zhao, R., Wang, X., Pan, C., Jiang, Y., Zhang, X., & Ge, B. (2022). Adsorption behavior and performance of ammonium onto sorghum straw biochar from water. Scientific Reports, *12*(1), 5358. https://doi.org/10.1038/s41598-022-08591-5

Zahra, M. B., Fayyaz, B., Aftab, Z.E.H., Akhter, A., Bahar, T., Anwar, W., & Haider, M. S. (2022). Characterization and utilization of cow manure biochar as soil amendment for the management of northern corn leaf blight. Journal of Soil Science and Plant Nutrition, *22*(3), 3348-3363. https://doi.org/10.1007/s42729-022-00891

Zhang, L., Guo, J., Huang, X., Wang, W., Sun, P., Li, Y., & Han, J. (2019). Functionalized biochar-supported magnetic MnFe 2 O 4 nanocomposite for the removal of Pb (ii) and Cd (ii). RSC Advances, *9*(1), 365-376. https://doi.org/10.1039/C8RA09061K

Zhang, M.-m., Liu, Y.-g., Li, T.-t., Xu, W.-h., Zheng, B.-h., Tan, X.-f., Wang, H., Guo, Y.-m, Guo, F. -y., & Wang, S.-f. (2015). Chitosan modification of magnetic biochar produced from Eichhornia crassipes for enhanced sorption of Cr (VI) from aqueous solution. RSC Advances, *5*(58), 46955-46964.

Zhao, M., Zou, G., Li, Y., Pan, B., Wang, X., Zhang, J., Xu, L., Li, C., & Chen, Y. (2025). Biodegradable microplastics coupled with biochar enhance Cd chelation and reduce Cd accumulation in Chinese cabbage. Biochar, *7*(1), 31. https://doi.org/10.1007/s42773-024-00418-y

Zhao, Q., Xu, T., Song, X., Nie, S., Choi, S.-E., & Si, C. (2021). Preparation and application in water treatment of magnetic biochar. Frontiers in Bioengineering and Biotechnology, *9*, 769667. https://doi.org/10.3389/fbioe.2021.769667